

Supplementary Information

The Critical Role of Isolated Ti^{3+} Sites in MIL-125 for Photocatalytic Nitrate Reduction: Performance Enhancement and Deactivation Mechanism

Lijun Liao,^{*a,c} Guangquan Zhao,^b Ruiwen Shu,^{*a} Xuepeng Wang,^b Jinxin Zhang^a and Ruting Yuan^{*b}

^a School of Chemical and Blasting Engineering, School of Earth and Environment, Anhui University of Science and Technology, Huainan, 232001, China

^b School of Chemistry and Chemical Engineering, Qilu University of Technology (Shandong Academy of Sciences), Jinan, Shandong, 250353, China

^c Hubei Key Laboratory of Novel Reactor and Green Chemical Technology, Wuhan Institute of Technology, Wuhan 430072, China

*Corresponding authors. Emails: lijun.liao@aust.edu.cn (Lijun Liao); rwshu@aust.edu.cn (Ruiwen Shu); rutingyuan@qlu.edu.cn (Ruting Yuan)

Characterizations

The powder X-ray diffraction (XRD) patterns were recorded using a Rigaku SmartLab SE X-ray diffractometer with a $\text{Cu K}\alpha$ X-ray source ($\lambda = 1.5406 \text{ \AA}$). Scanning electron microscopy (SEM) images were obtained with a Hitachi Regulus 8220 SEM, operating at 200-30 kV and a maximum current of 22 A during measurement. Transmission electron microscopy (TEM) was performed using a JEOL JEM-F200 microscope. UV-vis diffuse reflectance spectra (UV-Vis DRS) were collected on a PerkinElmer Lambda 1050+ spectrometer. Nitrogen adsorption-desorption isotherms were measured with a Micromeritics ASAP 2460 instrument, using the Brunauer–Emmett–Teller (BET) method. X-ray photoelectron spectroscopy (XPS) was performed using an ESCALAB Xi+ electron spectrometer (Thermo Fisher) equipped with a monochromatic X-ray source. Electron paramagnetic resonance (EPR) spectra were recorded using a Bruker EMXplus spectrometer. Mott-Schottky measurements of the samples were performed with a CHI 760E electrochemical workstation (Shanghai Chenhua Co., Ltd.), using a three-electrode setup and 0.2 M sodium sulfate as the electrolyte. Thermogravimetric analysis (TGA) profiles were recorded over a temperature range of 30-600 °C using a NETZSCH Thermal Analyzer (STA449 F3), with a heating rate of

5°/min in air flow.

Photocatalytic nitrate reduction to ammonia

Typically, 100 mg NaNO₃ was dissolved in 50 mL ultrapure water in a 100 mL quartz reactor. Then, 25 mg of catalyst was added to the above solution. The suspension was ultrasonically treated for 5 min before light irradiation by a 500 W Xenon Lamp (CEL-S500, Beijing China Education Au-light Co., Ltd.). The temperature of the reactant suspension was maintained at 25 °C during the experiment using a water cooling system. 5 mL of the reaction mixture was sampled from the reactor at intervals of 15 min, and the catalyst particles were removed using a syringe filter. The concentrations of NH₄⁺ in the reactant liquids were measured by Nessler's reagent test using a UV-9000 UV-Vis spectrometer from Shanghai Metash Instruments Co., Ltd. The obtained sample after 1 h reaction was washed with distilled water (DI) and methanol for at least 3 times, respectively, to remove the residual nitrate. The obtained sample was dried in an oven at 60 °C. For the cycling test, 100 mg NaNO₃, 25 mg MIL-125 catalyst, and 50 mL ultrapure water were mixed in a 100 mL quartz reactor and reacted for 1 h under full-spectrum light irradiation by a 500W Xenon Lamp. Then, 5 mL reactant liquid was collected for the NH₄⁺ test after each cycle, while the used catalysts were also collected and redispersed in fresh reactant containing 100 mg of NaNO₃ and 50 mL ultrapure water for the subsequent cycles. Five cycling reactions were performed, with each cycle lasting 1 h.

DFT calculations

All calculations were performed with periodic DFT using the Gaussian plane wave method implemented in CP2K's Quickstep module. The explorative studies of the catalysts structure were performed using the molecularly optimized basis set DZVP-MOLOPT-SR-GTH for each atom with a Goedecker-Teter-Hutter (GTH) pseudopotential. The calculations were conducted using the generalized gradient approximation and the Perdew-Burke-Ernzerhof (PBE) functional with DFT-D3 correction. An energy convergence for the self-consistent field (SCF) calculation was set to 3×10^{-6} Hartree. An energy cutoff of 400 Ry was used throughout the calculations. The different coordinator defect was crated via removing the BDF molecular in model. The input file was generated by Multiwfn.

The adsorption energies (E_{ads}) are calculated using the follow equation:

$$E_{ads} = E_{model + sub} - E_{model} - E_{sub}$$

where $E_{model+sub}$, E_{model} , and E_{sub} stand for the energy of adsorption configurations, the energy of

model, and the energy of adsorption molecular, respectively.

The NO₃RR process was calculated as fellow element step:

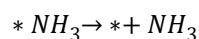
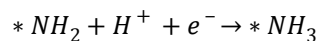
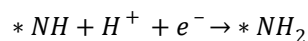
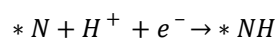
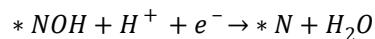
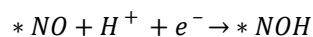
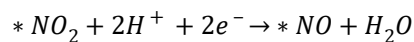
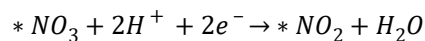
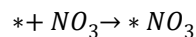


Table S1. Comparison of the photocatalytic ammonia synthesis efficiency between MIL-125 in this work and recently reported photocatalysts.

| Photocatalyst | Light source | Sacrificial agent | Optimal ammonia synthesis rate ($\mu\text{mol g}_{\text{cat}}^{-1} \text{h}^{-1}$) | Reference |
|---|------------------------------------|-------------------|--|-----------|
| BaO _{NC} -TiO ₂ | 300 W Xe lamp, full-spectrum | Ethylene glycol | 3500 | [1] |
| JRC-TIO-6 | 2 kW Xe lamp ($\lambda > 300$ nm) | Formic acid | 16 | [2] |
| Ag ₂ O/P25 | 300 W Hg lamp (365 nm) | Formic acid | 450 | [3] |
| Ru/g-C ₃ N ₄ | 300 W Xe lamp, full-spectrum | Formic acid | 150 | [4] |
| V _{Cu-S} rich CuIn ₂ S ₄ | 300 W Xe lamp | Ethylene glycol | 975.9 | [5] |
| CuO _x /TNS | 300 W Xe lamp | Formic acid | 6360 | [6] |
| Ni/H _x WO _{3-y} | 300 W Xe lamp, full-spectrum | Ethylene glycol | 10500 | [7] |

| | | | | |
|--|-------------------------------------|-----------------|--------|-----------|
| Cu-NM-1.5 | 300 W Xe lamp, full-spectrum | Ethylene glycol | 1929 | [8] |
| NVCN475 | 300 W Xe lamp ($\lambda > 420$ nm) | Formic acid | 8.83 | [9] |
| AgCu-CN | 300 W Xe lamp ($\lambda > 420$ nm) | Ethylene glycol | 630.5 | [10] |
| D-PDI | Not available | None | 149.6 | [11] |
| Pt SAs/Ti _{0.87} O ₂ NSs | LED (275 nm) | None | ca. 35 | [12] |
| Cu-TiO ₂ | 2 kW Xe lamp, AM 1.5G | None | 1.07 | [13] |
| β -FeOOH(Cl _T)-OVs | 2 kW Xe lamp ($\lambda > 300$ nm) | None | 9.5 | [14] |
| Au ₂ -COF | Xe lamp (AM 1.5) | None | 382.48 | [15] |
| Ru/MoO _{3-x} | 300 W Xe lamp | None | 370 | [16] |
| MIL-125 | 500 W Xe lamp, full-spectrum | None | 738.3 | This work |

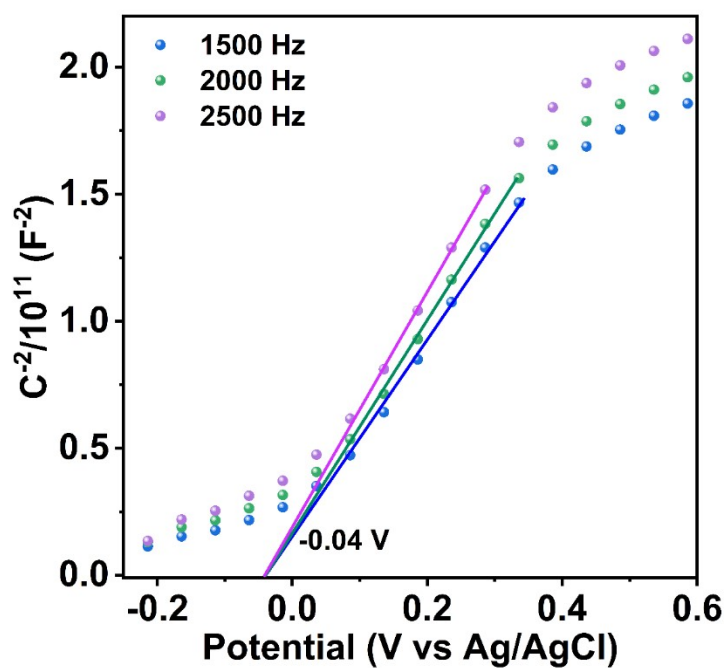


Figure S1. Mott-Schottky curves of MIL-125 after 1 h photocatalytic nitrate reduction reaction.

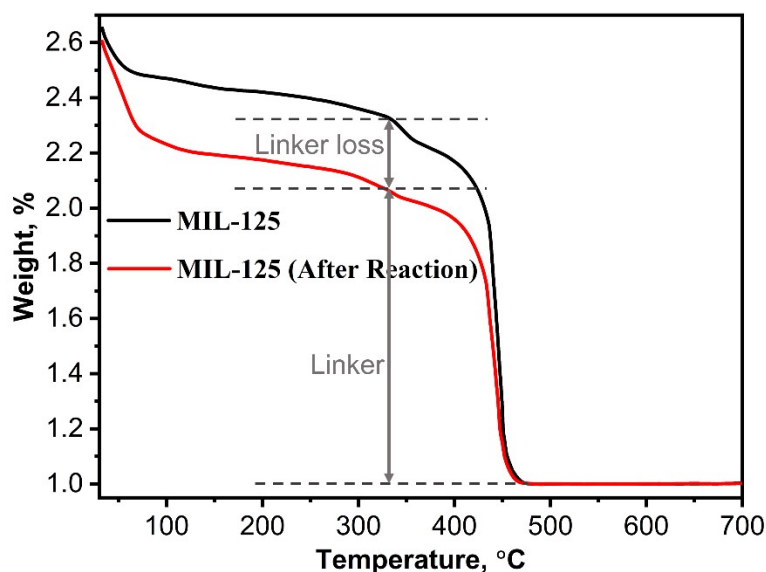


Figure S2. TGA curves of pristine MIL-125 and the MIL-125 after 1 h photocatalytic nitrate reduction reaction.

References

1. J. Li, R. Chen, J. Wang, Y. Zhou, G. Yang and F. Dong, *Nat. Commun.*, 2022, **13**, 1098.
2. H. Hirakawa, M. Hashimoto, Y. Shiraishi and T. Hirai, *ACS Catal.*, 2017, **7**, 3713-3720.
3. H.-T. Ren, S.-Y. Jia, J.-J. Zou, S.-H. Wu and X. Han, *Appl. Catal. B: Environ.*, 2015, **176-177**, 53-61.
4. D. Hao, J. Ren, Y. Wang, H. Arandiyani, M. Garbrecht, X. Bai, H. K. Shon, W. Wei and B.-J. Ni, *Energy Mater. Adv.*, 2021, **2021**, 9761263.
5. H. Liang, C. Ye, Y. Wu, J. Xiong, P. Zhang, X. Cao, G. Hao, W. Jiang and J. Di, *Appl. Catal. B: Environ. Energy*, 2025, **362**, 124776.
6. S. Shen, R. Chen, X. Li, J. Wang, S. Yu, J. Li and F. Dong, *Environ. Sci. Technol.*, 2024, **58**, 7653-7661.
7. Y. Wang, H. Yin, X. Zhao, Y. Qu, A. Zheng, H. Zhou, W. Fang and J. Li, *Appl. Catal. B: Environ.*, 2024, **341**, 123266.
8. Y. Zhao, J. Shen, J. Yuan, H. Mao, X. Cheng, Z. Xu and Z. Bian, *Nano Energy*, 2024, 109499.
9. I. Hong, H. S. Moon, B. J. Park, Y.-A. Chen, Y.-P. Chang, B. Song, D. Lee, Y. Yun, Y.-J. Hsu, J. W. Han and K. Yong, *Chem. Eng. J.*, 2024, **484**, 149506.
10. Z. Lian, D. Luo, J. Yang, Y. Yang, S. Tang, H. Li, D. Zhang and H. Li, *Angew. Chem. Int. Ed.*, 2026, **65**, e202516964.
11. H. Peng, Y. Liu, Y. Wang, M. Song, H. Song, P. Chen and S.-F. Yin, *ACS Catal.*, 2024, **14**, 2971-2980.
12. H. Jung, G. Cha, H. Kim, J. Will, X. Zhou, E. Spiecker, J. Breu and P. Schmuki, *J. Am. Chem. Soc.*, 2025, **147**, 9049-9055.
13. W. Hiramatsu, Y. Shiraishi, S. Ichikawa, S. Tanaka, Y. Kawada, C. Hiraiwa and T. Hirai, *J. Am. Chem. Soc.*, 2025, **147**, 1968-1979.
14. Y. Shiraishi, S. Akiyama, W. Hiramatsu, K. Adachi, S. Ichikawa and T. Hirai, *JACS Au*, 2024, **4**, 1863-1874.

15. X. Sun, J. Liu, Q. Li, C. Wang and B. Jiang, *Chin. J. Catal.*, 2025, **73**, 358-367.
16. L. Zhang, R. Li, L. Guo, L. Cui, X. Zhang, Y. Wang, Y. Wang, X. Jian, X. Gao, C. Fan, J. Wang and J. Liu, *ACS Catal.*, 2024, **14**, 5696-5709.